Cardiac arrhythmia in a mouse model of sodium channel *SCN8A* epileptic encephalopathy

Chad R. Frasier[a], Jacy L. Wagnon[b], Yangyang Oliver Bao[a], Luke G. McVeigh[a], Luis F. Lopez-Santiago[a], Miriam H. Meisler[b,c], and Lori L. Isom[a,c,d,1]

[a]Department of Pharmacology, University of Michigan, Ann Arbor, MI 48109; [b]Department of Human Genetics, University of Michigan, Ann Arbor, MI 48109; [c]Department of Neurology, University of Michigan, Ann Arbor, MI 48109; and [d]Department of Molecular and Integrative Physiology, University of Michigan, Ann Arbor, MI 48109

Edited by William A. Catterall, University of Washington School of Medicine, Seattle, WA, and approved September 27, 2016 (received for review August 4, 2016)

Patients with early infantile epileptic encephalopathy (EIEE) are at increased risk for sudden unexpected death in epilepsy (SUDEP). De novo mutations of the sodium channel gene *SCN8A*, encoding the sodium channel $Na_v1.6$, result in EIEE13 (OMIM 614558), which has a 10% risk of SUDEP. Here, we investigated the cardiac phenotype of a mouse model expressing the gain of function EIEE13 patient mutation p.Asn1768Asp in *Scn8a* ($Na_v1.6$-N1768D). We tested *Scn8a*$^{N1768D/+}$ mice for alterations in cardiac excitability. We observed prolongation of the early stages of action potential (AP) repolarization in mutant myocytes vs. controls. *Scn8a*$^{N1768D/+}$ myocytes were hyperexcitable, with a lowered threshold for AP firing, increased incidence of delayed afterdepolarizations, increased calcium transient duration, increased incidence of diastolic calcium release, and ectopic contractility. Calcium transient duration and diastolic calcium release in the mutant myocytes were tetrodotoxin-sensitive. A selective inhibitor of reverse mode Na/Ca exchange blocked the increased incidence of diastolic calcium release in mutant cells. *Scn8a*$^{N1768D/+}$ mice exhibited bradycardia compared with controls. This difference in heart rate dissipated after administration of norepinephrine, and there were no differences in heart rate in denervated ex vivo hearts, implicating parasympathetic hyperexcitability in the *Scn8a*$^{N1768D/+}$ animals. When challenged with norepinephrine and caffeine to simulate a catecholaminergic surge, *Scn8a*$^{N1768D/+}$ mice showed ventricular arrhythmias. Two of three mutant mice under continuous ECG telemetry recording experienced death, with severe bradycardia preceding asystole. Thus, in addition to central neuron hyperexcitability, *Scn8a*$^{N1768D/+}$ mice have cardiac myocyte and parasympathetic neuron hyperexcitability. Simultaneous dysfunction in these systems may contribute to SUDEP associated with mutations of *Scn8a*.

sodium channel | epilepsy | arrhythmia | channelopathy | mutation

$Na_v1.6$, encoded by *SCN8A*, is a major voltage-gated sodium channel (VGSC) in human brain (reviewed in ref. 1). $Na_v1.6$ is also expressed at low levels in mouse and human heart (2–6), where it is concentrated in the transverse tubules of ventricular myocytes and thought to regulate excitation–contraction coupling. De novo mutations of *SCN8A* are an important cause of early infantile epileptic encephalopathy (EIEE) type 13 [Online Mendelian Inheritance in Man (OMIM) 614558]. The first pathogenic mutation of *SCN8A*, p.Asn1768Asp, was identified in a proband with onset of convulsive seizures at 6 mo of age (7). Comorbidities included intellectual disability, ataxia, and sudden unexpected death in epilepsy (SUDEP) at 15 y of age. Since then, more than 140 patients with *SCN8A* mutations have been identified (8) (www.SCN8A.net/Home.aspx). The combined incidence of de novo mutations of *SCN8A* in EIEE was 1% (19 of 1,957) in five large studies of several hundred individuals each (9–13). Common features of EIEE13 include seizure onset between birth and 18 mo of age, mild to severe cognitive and developmental delay, and mild to severe movement disorders that may result in immobility (8). Approximately 10% (5 of 43) of reported cases with clinical description experienced SUDEP during childhood or adolescence (7, 10, 14, 15).

All of the *SCN8A* mutations in EIEE13 are missense mutations, with the single exception of a splice site mutation that results in an in-frame deletion; protein truncation mutations have not been observed. Ten EIEE13 mutations have been subjected to functional tests in transfected cells, and 8 of 10 conferred gain of function changes in biophysical properties of $Na_v1.6$ that are predictive of neuronal hyperexcitability, including elevated persistent sodium current ($I_{Na,\ P}$), hyperpolarizing shifts in voltage dependence of current activation, and impaired current inactivation (7, 14, 16–18). Analysis of neuronal function in a mouse model confirmed increased $I_{Na,\ P}$ and neuronal hyperexcitability in vivo for one of the mutations (19, 20).

Risk factors for SUDEP include early age of seizure onset and high frequency of pharmacoresistant seizures (21), both characteristic of EIEE13 patients. In the related Dravet syndrome (EIEE6; OMIM 607208), primarily caused by mutations in the VGSC gene *SCN1A*, ∼15% of patients die from SUDEP (22). In mouse models of Dravet syndrome, SUDEP seems to result from a combination of altered excitability in brain, autonomic nervous system, and heart (23, 24). Another Dravet syndrome model, the *Scn1b* null mouse, also exhibits a neurocardiac mechanism of SUDEP (25, 26).

To investigate the pathogenic effects of *SCN8A*-linked EIEE13, we generated a knock-in mouse carrying the original patient mutation p.Asn1768Asp (N1768D) (27). In transfected neurons, this mutation generated elevated $I_{Na,\ P}$ and neuronal hyperexcitability (7). Heterozygous *Scn8a*$^{N1768D/+}$ mice recapitulate

Significance

Patients with epileptic encephalopathy have a high risk of sudden unexpected death in epilepsy (SUDEP), an event described as arrhythmia of brain and heart. We investigated the cardiac phenotype of a model of an epileptic encephalopathy caused by mutation of sodium channel *SCN8A*. We observed that mutant heart cells were hyperexcitable, exhibiting abnormal contraction and action potential wave forms. Mutant mice also had reduced heart rates compared with controls. This difference in heart rate was not observed in isolated hearts, implicating changes in cardiac regulation by the parasympathetic nervous system. When challenged with norepinephrine and caffeine, mutant mice had ventricular arrhythmias. These cardiac and parasympathetic abnormalities are predicted to contribute to the mechanism of SUDEP in patients with *SCN8A* mutations.

Author contributions: C.R.F., M.H.M., and L.L.I. designed research; C.R.F., J.L.W., Y.O.B., L.G.M., and L.F.L.-S. performed research; C.R.F., J.L.W., Y.O.B., and L.F.L.-S. analyzed data; and C.R.F., J.L.W., M.H.M., and L.L.I. wrote the paper.

The authors declare no conflict of interest.

This article is a PNAS Direct Submission.

[1]To whom correspondence should be addressed. Email: lisom@umich.edu.

This article contains supporting information online at www.pnas.org/lookup/suppl/doi:10.1073/pnas.1612746113/-/DCSupplemental.

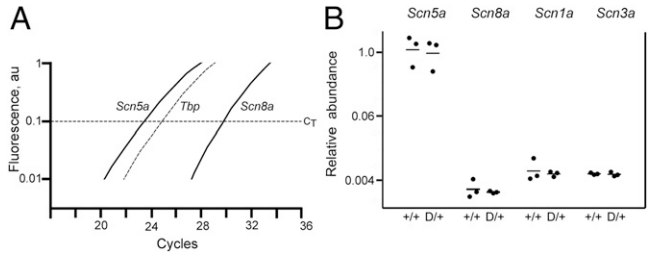

Fig. 1. Quantification of VGSC transcripts in heart RNA by quantitative RT-PCR. (*A*) Representative traces show that amplification of the *Scn5a* transcript requires fewer PCR cycles than amplification of the *Scn8a* transcript. (*B*) Data corrected for amplification of the internal control, Tbp. Transcript abundance does not differ between mutant and WT mice. The abundance of transcripts of three TTX-S channels *Scn1a*, *Scn3a*, and *Scn8a* is comparable. Together, they are ~1% of the total VGSCs in heart. Each symbol represents RNA from one animal. D/+, $Scn8a^{N1768D/+}$ ($n = 3$); +/+, $Scn8a^{+/+}$ ($n = 3$).

the seizures, ataxia, and sudden death of the heterozygous proband, with seizure onset at 2–4 mo of age and progression to death within 30 d (28). We hypothesized that gain of function mutations of *SCN8A* in patients with EIEE13 could cause cardiac arrhythmias in addition to neuronal hyperexcitability, contributing to SUDEP risk. Our results here suggest that *Scn8a* plays a vital role in both neuronal and cardiac excitability in mice and provide information on altered cardiac and parasympathetic excitability that may underlie SUDEP in human EIEE.

Methods

Detailed methods can be found in *SI Methods*.

Animals. $Scn8a^{N1768D}$ knock-in mice were generated as described and maintained on the C57BL/6J strain background (27, 28). All experiments were performed in accordance with the NIH guidelines, with approval from the University of Michigan Institutional Animal Care and Use Committee.

Quantitative RT-PCR. Total RNA was isolated from three $Scn8a^{N1768D/+}$ mutant mice and three $Scn8a^{+/+}$ controls (WT) at 3 mo of age. Each sample was assayed in quadruplicate. Transcripts of *Scn1a*, *Scn3a*, *Scn8a*, and *Scn5a* were measured with Taqman assays Mm00450580, Mm00658167, Mm00488119, and Mm00451971, respectively. Transcripts of the TATA binding protein (Tbp) were measured with Taqman assay Mm00446971 and served as internal controls. Δthreshold cycle (Ct) was calculated as cycles to reach threshold for the Tbp transcript minus cycles to reach threshold for the VGSC transcript.

Action Potential Recordings. Mouse ventricular myocytes were acutely dissociated using published methods (23). Only rod-shaped myocytes with a diastolic membrane potential more negative than −65 mV were used for analysis.

Intracellular Calcium Imaging. After dissociation, ventricular myocytes were loaded with 5 μM Fluo-4AM (Life Technologies). Myocytes were field stimulated at 0.5 Hz using extracellular platinum electrodes.

Sodium Current Recordings. Voltage clamp recordings were performed at room temperature as described (23, 25). P/4 leak subtraction was used where appropriate to accurately determine $I_{Na,\ P}$.

Myocyte Contraction. To assess the contractility of individual myocytes, dissociated cells were imaged on an IonOptix Microscope (IonOptix) and paced from 0.5 to 4 Hz in ascending fashion. Data are presented at 0.5 Hz. Myocyte contractility was determined using edge detection.

ECG Recordings. For in vivo ECG recordings in anesthetized mice, an i.p. injection of 2 mg/kg norepinephrine (NE) was used to assess response to a sympathetic agonist. Twenty minutes later, 120 mg/kg caffeine was injected i.p. to simulate a catecholaminergic surge and assess the incidence of ventricular arrhythmias (29, 30). For ex vivo experiments, pseudo-ECGs were recorded from isolated Langendorff-perfused mouse hearts using published methods (4, 23, 26).

Radiotelemetry ECG Recordings. Three WT and three $Scn8a^{N1768D/+}$ mice (age postnatal day 60) were implanted with radiotelemetry ECG devices (DSI) by the University of Michigan Physiology Phenotyping Core as described (23).

Statistical Analyses. Results are expressed as mean ± SEM. Where appropriate, Student's *t* test or χ^2 was used to compare WT and $Scn8a^{N1768D/+}$ animals. Statistical significance was achieved when $P < 0.05$. The number of animals in each experiment is represented as *N*. The number of cells in each experiment is represented as *n*.

Results

***Scn8a* Is Expressed in Cardiac Tissue of Adult Mice.** We used a Taqman assay that detects transcripts encoding the full-length $Na_v1.6$ protein but not the alternatively spliced transcript encoding a truncated protein (31, 32). Cardiac RNA from three WT and three $Scn8a^{N1768D/+}$mutant mice was analyzed. Amplification of transcripts from the major cardiac sodium channel, *Scn5a*, required fewer PCR cycles than the *Scn8a* transcript (Fig. 1*A*). The difference in abundance between *Scn5a* and *Scn8a* in heart corresponds to eight PCR cycles (Fig. 1*B*). The abundance of the *Scn8a* transcript is, thus, 2^8 or 250-fold lower than *Scn5a*. *Scn1a* and *Scn3a* are also expressed at low levels in heart (33). The levels of *Scn1a* and *Scn3a* transcripts are similar to *Scn8a* transcripts (Fig. 1*B*). Together, the three tetrodotoxin-sensitive (TTX-S) channels account for ~1% of VGSC transcripts in heart.

To detect potential transcriptional compensation for the $Scn8a^{N1768D}$ mutation in vivo, we also compared the abundance of VGSC transcripts in mutant and WT heart. *Scn1a*, *Scn3a*, *Scn5a*, and *Scn8a* transcripts did not differ in abundance between $Scn8a^{+/+}$ and $Scn8a^{N1768D/+}$ mice (Fig. 1*B*). Thus, the gain of function mutation of *Scn8a* does not lead to compensatory changes in its own transcription or transcription of the other VGSCs in heart.

Ventricular Myocyte Morphology. Myocyte length and width were previously found to be reduced in $Scn8a^{-/-}$ null mice (4). We, therefore, assessed myocyte morphology in $Scn8a^{N1768D/+}$ mice. Images of freshly isolated ventricular myocytes were acquired within 1 h postisolation. We found no difference in cell length or width between mutant and WT cells (Table S1). There were also no differences in cell capacitance measured in patch clamp experiments (Table S1), indicating no differences in cell volume.

No Differences in Sodium Current of Ventricular Myocytes. We observed no effects of the N1768D mutation on whole-cell transient sodium current (I_{Na}), $I_{Na,\ P}$, or the voltage dependence of activation and inactivation of I_{Na} (Table S2). This result is consistent with the data indicating that $Na_v1.5$ transcripts are 99% of cardiac VGSC transcripts in mutant and WT mice (Fig. 1). This

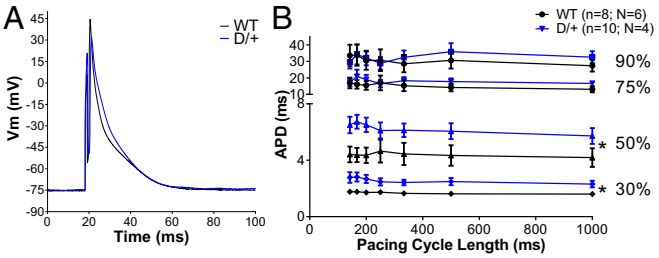

Fig. 2. $Scn8a^{N1768D/+}$ myocytes have altered AP morphology. (*A*) Representative traces from WT (black) and $Scn8a^{N1768D/+}$ (red) ventricular myocytes. (*B*) The early stages of repolarization (APD_{30} and APD_{50}) are significantly prolonged in $Scn8a^{N1768D/+}$ myocytes compared with WT ($P = 0.01$ and $P = 00.04$, respectively). The total APD, APD_{90}, is not altered ($P = 0.41$). $Scn8a^{N1768D/+}$ (D/+): $n = 10$, $N = 4$; and $Scn8a^{+/+}$ (WT): $n = 8$, $N = 6$. V_m, membrane potential. *$P < 0.05$ vs. WT.

result is also consistent with previous reports that less than 10% of the whole-cell I_{Na} is TTX-S (3, 34).

Altered Action Potential Morphology and Delayed Afterdepolarizations in *Scn8a*$^{N1768D/+}$ Mice. To assess the effect of the p.Asn1768Asp mutation on cardiac excitability, we recorded ventricular myocyte action potentials (APs) under current clamp. The duration of the early phases of AP repolarization [action potential duration (APD); APD_{30} and APD_{50}] was prolonged in *Scn8a*$^{N1768D/+}$ myocytes (Fig. 2, red), with no difference in total duration (Fig. 2). Myocytes from *Scn8a*$^{N1768D/+}$ mice had a lower current threshold for AP firing (Fig. 3*C*). We also observed an increased incidence of delayed afterdepolarizations (DADs) in *Scn8a*$^{N1768D/+}$ myocytes, suggesting the existence of arrhythmogenic substrates (Fig. 3 *A* and *B*). Importantly, we observed no difference in the resting membrane potential, AP peak, or AP upstroke velocity (Table S3), indicating that the observed hyperexcitability of *Scn8a*$^{N1768D/+}$ myocytes was not caused by depolarized cells or compensatory changes in $Na_v1.5$ expression, which is in agreement with Fig. 1*B* and Table S2.

Prolonged Calcium Transient Duration and Increased Incidence of Diastolic Calcium Release. The prolongation of the early stages of the AP in *Scn8a*$^{N1768D/+}$ myocytes (Fig. 2) suggested the possibility of altered intracellular calcium handling. The duration of the calcium transient was significantly prolonged in *Scn8a*$^{N1768D/+}$ myocytes (Fig. 4*A*, blue, and *C*). In agreement with the increased incidence of DADs in mutant mice (Fig. 3*A*), we observed an increase in the incidence of aberrant diastolic calcium release (DCR) events (Fig. 4*D*). These excess DCR events in *Scn8a*$^{N1768D/+}$ myocytes occurred in the intervals between pacing stimuli and also, after cessation of pacing (Fig. 4*B*, *Left*). In the majority of cells, these calcium waves were stable and persisted long after pacing was terminated (Fig. 4*B*, *Left*). Myocytes were treated with 100 nM TTX, a concentration that selectively inhibits TTX-S VGSCs, including $Na_v1.6$, but does not inhibit the tetrodotoxin-resistant (TTX-R) VGSC $Na_v1.5$. In the presence of 100 nM TTX, both the calcium transient duration and the incidence of DCR events in mutant myocytes are returned to WT levels, showing that a TTX-S current, likely through mutant $Na_v1.6$ channels, is responsible for both abnormalities (Fig. 4*B*, *Right*, *C*, and *D*). Treatment with 5 μM SN-6, a selective inhibitor of reverse mode Na/Ca exchange, blocked the increased incidence of DCR in mutant myocytes with no effect on duration of the calcium transient (Fig. 4 *C* and *D*). To rule out other sources of aberrant calcium release, we tested possible differences in sarcoplasmic reticulum (SR) leak or SR load. We observed no differences in SR leak (Fig. 4*E*) or SR load (Fig. 4*F*) between genotypes. Taken together, these data are consistent with a model in which increased TTX-S $I_{Na,\ P}$ at the t-tubules results in increased probability of calcium influx through reverse mode Na/Ca exchange, leading to cellular hyperexcitability.

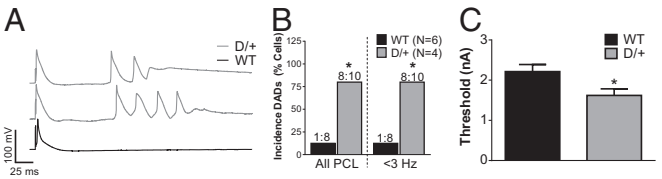

Fig. 3. *Scn8a*$^{N1768D/+}$ myocytes are hyperexcitable and display increased arrhythmogenecity. (*A*) Representative traces of DADs recorded in *Scn8a*$^{N1768D/+}$ myocytes (gray) compared with WT (black). (*B*) The incidence of DADs was significantly increased in *Scn8a*$^{N1768D/+}$ animals compared with WT ($P = 0.001$). (*C*) *Scn8a*$^{N1768D/+}$ myocytes have a significant reduction in AP threshold ($P = 0.03$). For *B* and *C*, *Scn8a*$^{N1768D/+}$ (D/+): $n = 10$, $N = 4$; *Scn8a*$^{+/+}$ (WT): $n = 8$, $N = 6$. PCL, pacing cycle length. $^*P < 0.05$ vs. WT.

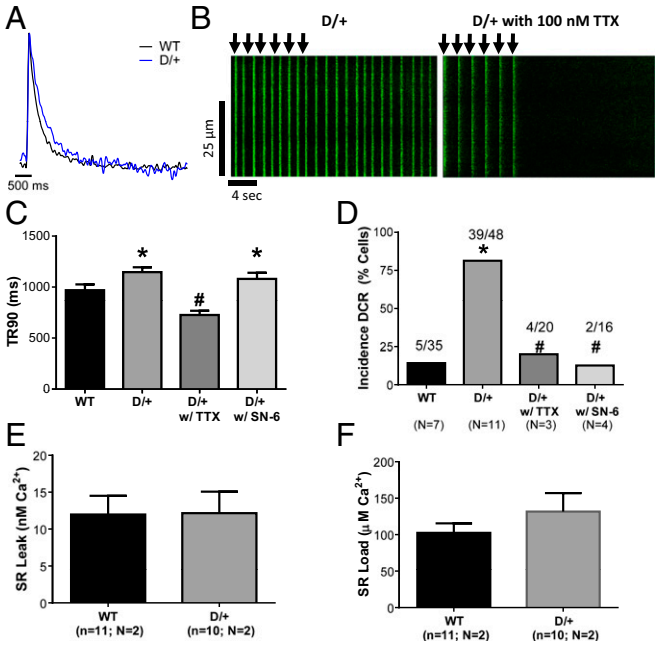

Fig. 4. *Scn8a*$^{N1768D/+}$ myocytes have increased calcium transient duration and increased incidence of calcium waves. (*A*) Overlay of calcium transients from WT (black) and *Scn8a*$^{N1768D/+}$ (blue). (*B*) Representative line scans from *Scn8a*$^{N1768D/+}$ myocytes (*Left*) before and (*Right*) after application of 100 nM TTX. Cells were paced at 0.5 Hz for six beats (arrows). In the absence of TTX, calcium waves occur between the pacing stimuli, which are marked by arrows, and continue after pacing is terminated. In the presence of 100 nM TTX to inhibit TTX-S VGSCs, including $Na_v1.6$, the normal 1:1 relationship between pacing stimuli and calcium waves is restored, showing the contribution of the mutant channel. (*C*) *Scn8a*$^{N1768D/+}$ myocytes have increased calcium transient duration ($P = 0.01$ vs. WT), which is returned to control levels in the presence of 100 nM TTX ($P < 0.001$ vs. *Scn8a*$^{N1768D/+}$) but unaffected by 5 μM SN-6 ($P = 0.43$ vs. *Scn8a*$^{N1768D/+}$). $^*P < 0.05$ vs. WT; $^{\#}P < 0.05$ vs. D/+ as well as vs. WT. (*D*) The incidence of DCR events is increased in *Scn8a*$^{N1768D/+}$ myocytes ($P < 0.001$ vs. WT) and returned to control levels by the addition of 100 nM TTX or 5 mM SN-6 ($P < 0.001$ vs. untreated *Scn8a*$^{N1768D/+}$ for both drug treatments). $^*P < 0.05$ vs. WT; $^{\#}P < 0.05$ vs. D/+. (*E*) No differences were observed in the amount of SR leak between genotypes ($P = 0.96$). (*F*) No differences were observed in the amount of SR load between genotypes ($P = 0.31$). In *C* and *D*, *Scn8a*$^{+/+}$ (WT): $n = 35$, $N = 7$; *Scn8a*$^{N1768D/+}$ (D/+): $n = 48$, $N = 11$; D/+ with TTX: $n = 20$, $N = 3$; and D/+ with SN-6: $n = 16$, $N = 4$. In *E* and *F*, WT: $n = 11$, $N = 2$; and D/+, $n = 10$, $N = 2$. No significant differences between genotypes. TR90, transient duration to 90%.

Ectopic Beating in *Scn8a*$^{N1768D/+}$ Myocytes. During normal cardiac function, myocytes contract in response to increased intracellular calcium. Because of the significant differences in calcium transient duration between *Scn8a*$^{N1768D/+}$ and WT myocytes, we examined myocyte contractility. In agreement with our cell morphology data, we found no differences in myocyte length or changes in cell length during contractility (Fig. 5*B* and Table S4). This result indicates that, despite prolonged calcium transients, *Scn8a*$^{N1768D/+}$ myocytes are not hypercontractile. Consistent with the lack of difference in total APD, there was no difference in cellular relaxation time after contraction (Fig. 5*C*) and no difference in the maximal rate of contraction or relaxation between genotypes (Table S4). In contrast and consistent with the high rate of DADs and DCR, we observed a higher incidence of ectopic beats between stimuli in *Scn8a*$^{N1768D/+}$ myocytes (Fig. 5 *A* and *D*).

***Scn8a*$^{N1768D/+}$ Mice Exhibit Bradycardia and Ventricular Arrhythmias in Vivo.** Surface ECGs of anesthetized *Scn8a*$^{N1768D/+}$ and WT mice were assessed in vivo. We observed decreased heart rate, or

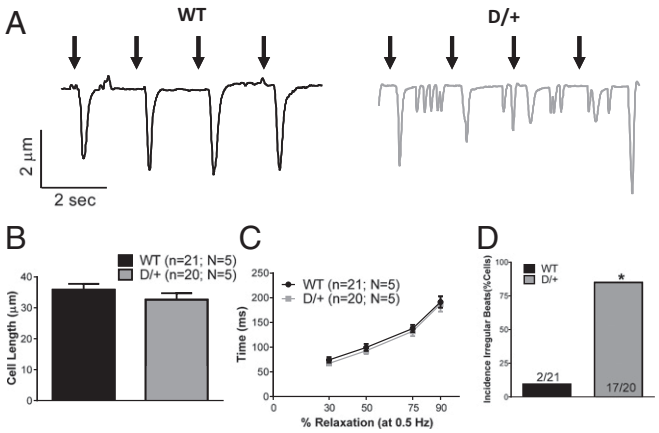

Fig. 5. Working myocytes from *Scn8a*$^{N1768D/+}$ mice display hyperexcitability and ectopic beating. (*A*) Representative traces from WT (black) and *Scn8a*$^{N1768D/+}$ (gray) myocytes. Black arrows represent pacing stimulus. No differences in (*B*) cell length ($P = 0.72$) or (*C*) relaxation times ($P = 0.36$) were observed. (*D*) Increased incidence of irregular beats in *Scn8a*$^{N1768D/+}$ mice ($P < 0.001$). Data are presented at 0.5 Hz. *Scn8a*$^{+/+}$ (WT): $n = 21$, $N = 5$; *Scn8a*$^{N1768D/+}$ (D/+): $n = 20$, $N = 5$. *$P < 0.05$ vs. WT.

bradycardia, in *Scn8a*$^{N1768D/+}$ animals (Fig. 6*A*, *Left*), suggesting parasympathetic hyperexcitability. There were no significant differences in ECG waveform properties between genotypes (Table S5), suggesting that observed heart rate differences were not caused by impaired conduction or repolarization in *Scn8a*$^{N1768D/+}$ animals.

To evaluate sympathetic/parasympathetic balance, we administered 2 mg/kg sympathetic agonist NE. As expected, this treatment resulted in increased heart rate in mice of both genotypes. The maximal heart rate after NE injection did not differ between groups (Fig. 6*A*, *Right*).

To determine whether the observed bradycardia in intact animals was caused by alterations in the autonomic nervous system or altered automaticity of the heart, we performed experiments in denervated Langendorff-perfused hearts. Using this method, we found no differences between genotypes (Fig. 6*B*), further suggesting that the reduced in vivo heart rate is caused by parasympathetic hyperexcitability in *Scn8a*$^{N1768D/+}$ mice.

The isolated ventricular myocyte recordings (Figs. 2–5) suggested the presence of arrhythmogenic substrates in *Scn8a*$^{N1768D/+}$ mice. Previous work indicated that changes in autonomic tone may precede SUDEP in patients (35–37) and mice (24). We simulated a catecholaminergic surge by i.p. administration of 120 mg/kg caffeine 20 min after the 2-mg/kg NE injection. At the time of caffeine injection, the heart rate in both genotypes remained at the plateau of the NE response. Caffeine administration resulted in multiple premature ventricular contractions and short runs of tachycardia in *Scn8a*$^{N1768D/+}$ mice (Fig. 6*C*) but not in WT mice, supporting our hypothesis that *Scn8a*$^{N1768D/+}$ hearts contain arrhythmogenic substrates.

Severe Bradycardia Precedes Death in *Scn8a*$^{N1768D/+}$ Animals. We implanted radio telemeters in three mutant mice and two WT mice and measured ECGs in freely moving animals for up to 60 d. The telemetry recordings captured terminal events in two *Scn8a*$^{N1768D/+}$ animals. In both animals, heart rate began to decrease ~36 h before death (Fig. 7) and remained depressed leading up to asystole. In one of the mutants, atrioventricular (AV) block was observed 1 h preceding death and continued to worsen until asystole (Fig. 7*A*, *Inset*). The third *Scn8a*$^{N1768D/+}$ animal survived the 60-d recording period. One WT animal became moribund after implant surgery and was euthanized; the other survived the 60-d recording period.

Discussion

Early mortality caused by SUDEP is a major concern for EIEE families (38, 39). Indirect evidence has linked SUDEP to seizure-induced apnea, pulmonary edema, dysregulation of cerebral circulation, autonomic dysfunction, and cardiac arrhythmias (40–44). In this study, we show that disturbances in cardiac and parasympathetic excitability contribute to the mechanism of death in a mouse model of EIEE13. Cardiac myocytes from *Scn8a*$^{N1768D/+}$ mice are hyperexcitable, exhibiting prolongation of the early phases of AP repolarization, lowered threshold for AP firing, and increased incidence of DADs. These observations provide a demonstration of pathogenic consequences of expression of mutant $Na_v1.6$ in the heart. Quantitation of transcript levels indicates that $Na_v1.6$ is expressed at only 0.4% of the level of the major cardiac channel $Na_v1.5$, but its localized subcellular concentration in transverse tubules (t-tubules) (4) results in significant functional consequences. Consistent with increased $I_{Na,\ P}$ in the t-tubules, we observed arrhythmogenic substrates, including elevated calcium transient duration, increased incidence of calcium waves, and increased incidence of ectopic beats, in *Scn8a*$^{N1768D/+}$ myocytes. At the whole-animal level, bradycardia and ventricular arrhythmias were recorded using surface ECG measurements in anesthetized mice, and severe bradycardia preceded asystole and death in freely moving animals under telemetry. Overall, these data suggest that EIEE13

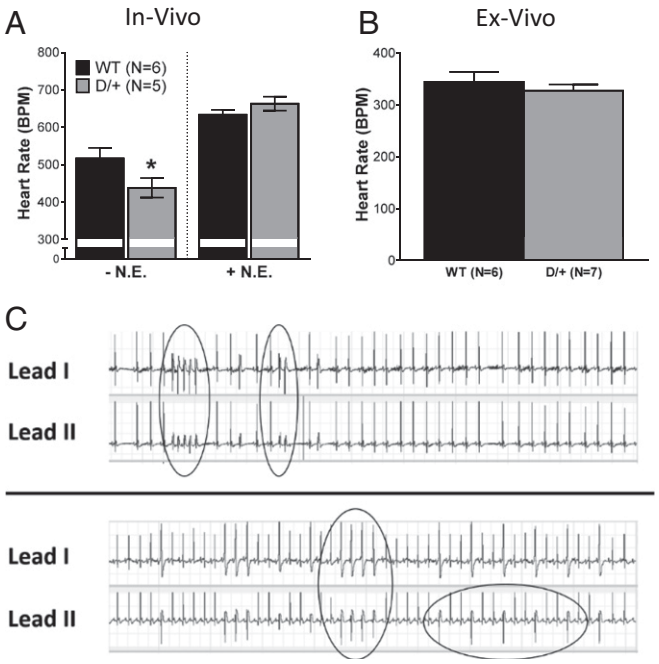

Fig. 6. *Scn8a*$^{N1768D/+}$ mice display characteristics of increased parasympathetic activity and cardiac arrhythmias in vivo. (*A*) Anesthetized *Scn8a*$^{N1768D/+}$ mice have significantly decreased heart rates (HR, in beats per minute, BPM) compared with WT as assessed by surface ECG ($P = 0.03$). Administration of 2 mg/kg i.p. NE eliminates this difference ($P = 0.39$). (*B*) Denervated ex vivo heart preparations show no differences in heart rate between groups ($P = 0.45$). (*C*) Representative surface ECG recording of arrhythmogenic events recorded in two anesthetized *Scn8a*$^{N1768D/+}$ mice after injection of 2 mg/kg i.p. NE and 120 mg/kg i.p. caffeine. Episodes of ventricular tachycardia and premature ventricular beats are circled in the traces. *Scn8a*$^{+/+}$ (WT): $n = 6$; and *Scn8a*$^{N1768D/+}$ (D/+): $n = 5$ for in vivo studies. WT: $n = 6$; and D/+: $n = 7$ for ex vivo studies. *$P < 0.05$ vs. WT.

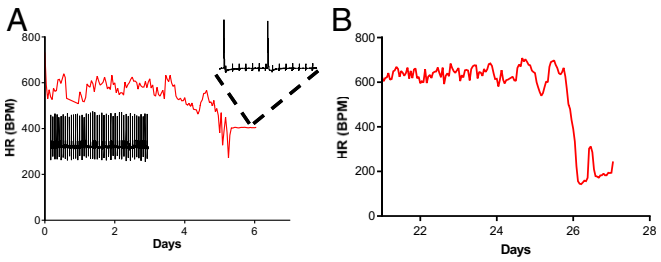

Fig. 7. Bradycardia precedes death in *Scn8a*$^{N1768D/+}$ mice. Heart rate (HR, in beats per minute, BPM) preceding asystole and death is shown for two *Scn8a*$^{N1768D/+}$ mice. (*A*) HR began to decline ~36 h before asystole (arrow) followed by severe AV block 1 h before asystole (*Inset*). (*B*) Severe bradycardia (~150 BPM) for 36 h preceding asystole (arrow).

patients with gain of function mutations in *SCN8A* may experience ventricular arrhythmias in addition to seizures. Furthermore, this work suggests that a combination of bradycardia and parasympathetic hyperexcitability may contribute to terminal SUDEP events in EIEE13 patients.

The phenotype of the *Scn8a*$^{N1768D/+}$ EIEE13 mouse model overlaps partially with that of *Scn1b* null mice (25, 26), a model of a rare form of Dravet syndrome. In both cases, prolonged calcium transients are secondary to TTX-S I_{Na} in cardiac myocytes. Our data also overlap with the *Scn1a*$^{+/-}$ Dravet syndrome mouse model, in which death is proposed to arise from postictal increased parasympathetic activity leading to atrioventricular nodal block and lethal bradycardia (24). Because $Na_v1.6$ is expressed in peripheral nerves (1), it is not surprising to find evidence of altered parasympathetic activity in *Scn8a*$^{N1768D/+}$ mice. In contrast to the Dravet syndrome models (23, 25, 26), cardiac arrhythmia in *Scn8a*$^{N1768D/+}$ mice does not involve altered expression of other VGSC genes or changes in whole-cell I_{Na}.

Channelopathies have been described as "electrical storms in the brain and the heart" (45). Overlapping neuronal and cardiac expression patterns of mutant ion channels are proposed to underlie the pathophysiology of a number of genetic diseases that exhibit both epilepsy and cardiac arrhythmia. In addition to mutations in genes encoding VGSC α- and β-subunits, mutations in the neurocardiac potassium channel genes *KCNA1* (46, 47), *KCNH2* (48–51), *KCNQ1* (52), and *KCNT1* (53) as well as *HCN1* (54, 55) have been linked to SUDEP. Mutations in genes encoding proteins that modify ion channels in brain and heart, such as *SENP-2*, also lead to SUDEP in animal models (56).

In partial agreement with our work on genetic models here and in previous studies (23, 25, 26), a recent study of a rat kainate model of epilepsy observed prolongation of ventricular APs (57). In contrast to our data, these investigators found an increased contribution of TTX-S VGSCs to whole-cell cardiac I_{Na} and $I_{Na,\,P}$ after kainate treatment. Taken together, these studies suggest that TTX-S VGSCs play important roles in cardiac APD and that SUDEP may involve elevated TTX-S channel activity in the heart. Thus, an emerging theme in the mechanism of SUDEP is aberrant cardiac and parasympathetic excitability driven, in part, by TTX-S VGSCs. Until recently, the functional role of TTX-S VGSCs in the heart was a point of debate. Early work showed that perfusion of low concentrations of TTX in isolated heart preparations slowed contraction and relaxation (3, 58). Several studies subsequently showed that TTX-S VGSCs are highly enriched in the t-tubules of ventricular myocytes (4, 34, 59) but largely absent from the lateral membrane and intercalated disk (26). T-tubules are sites of calcium-induced calcium release that ultimately lead to myocyte contraction. TTX-S VGSCs colocalize with ryanodine receptors in this subcellular domain (60). Recently, calcium-induced calcium release at the t-tubules was shown to be affected by TTX-S VGSC activity (61). Finally, in a mouse model of polymorphic ventricular tachycardia caused by dysregulated RyR2 channels, catecholamines were shown to promote aberrant DCR via increased TTX-S VGSC (likely $Na_v1.6$)-mediated $I_{Na,\,P}$ (60).

This study shows that a gain of function mutation in $Na_v1.6$ results in hyperexcitability and abnormal calcium cycling in cardiac myocytes that may provide a substrate for arrhythmogenesis. We propose that increased TTX-S $I_{Na,\,P}$ conducted by mutant $Na_v1.6$ channels in the t-tubules prolongs the early phases of the AP that may result in reverse mode Na/Ca exchange. Increased calcium influx would then lead to increased incidence of DCR and DADs. Increased susceptibility to arrhythmogenic events at the cellular level may be further potentiated by increased adrenergic stimulation, which is often observed in human patients after seizures (62). Others have shown that isoproterenol can increase $I_{Na,\,P}$ in the heart (63, 64). This result may explain our observation that arrhythmias can be induced in *Scn8a*$^{N1768D/+}$ mice under simulated catecholaminergic stress, which may increase an already elevated level of $I_{Na,\,P}$. Interestingly, we observe prolongation of calcium transients in the absence of changes to myocyte size or relaxation kinetics. These data suggest that intracellular calcium levels may remain elevated in the space surrounding the t-tubular membrane, away from the myofilaments. In view of the increased incidence of ectopic beats in *Scn8a*$^{N1768D/+}$ mice, calcium influx through reverse mode Na/Ca exchange may be sufficient to cause calcium-induced calcium release. The proposed increase in intracellular Na^+ in this space in the mutant mice, because of increased $I_{Na,\,P}$, may reduce the driving force of calcium extrusion by the Na/Ca exchanger.

In both cardiac and neuronal APs, excitation relies heavily on I_{Na}. It is consistent that animals with mutations in VGSC genes that are expressed in brain, autonomic neurons, and heart, such as *SCN8A*, exhibit both epilepsy and cardiac arrhythmia and that neurocardiac mechanisms underlie SUDEP. Acutely dissociated hippocampal neurons from *Scn8a*$^{N1768D/+}$ mice have elevated $I_{Na,\,P}$ and are hyperexcitable, and hippocampal neurons in *Scn8a*$^{N1768D/+}$ brain slices display ectopic firing patterns with early afterdepolarization-like events, in which multiple APs are elicited from a single stimulus (19, 20). Although not identical, this neuronal AP firing pattern is similar to the DADs observed here in *Scn8a*$^{N1768D/+}$ cardiomyocytes (Fig. 3) and suggests that the underlying mechanisms of epilepsy and cardiac arrhythmia may share similar components.

In conclusion, although seizures can trigger cardiac events indirectly through stimulation of the autonomic nervous system, our prior work and this work show that mutations of three VGSC genes, *Scn1a*, *Scn1b*, and *Scn8a*, all result in intrinsic alteration of cardiac myocyte excitability. These mutations also seem to alter the excitability of neurons in the parasympathetic system. Both effects may act as substrates for initiation of cardiac arrhythmias, with parasympathetic hyperexcitability ultimately resulting in bradycardia, asystole, and SUDEP in EIEE patients. In support of this hypothesis, a patient with an *SCN8A*-linked EIEE13 mutation was recently reported to experience cardiac arrhythmias and ictal asystole (65). Our work suggests that better monitoring of cardiac function in EIEE patients with mutations of *SCN1A*, *SCN1B*, and *SCN8A* may be an effective strategy for reducing SUDEP risk.

ACKNOWLEDGMENTS. We thank Robert Hurst for assistance with data analysis. This work was supported by NIH Grants T32 HL007853 (to C.R.F.; postdoctoral funding), UL1 TR000433 (to C.R.F.; postdoctoral funding), R01 NS034509 (to M.H.M.), R01 NS076752 (to L.L.I.), U01 NS090364 (to L.L.I.), and CURE 351092 (to L.L.I.) and a Postdoctoral Fellowship from the Dravet Syndrome Foundation (J.L.W.).

1. O'Brien JE, Meisler MH (2013) Sodium channel SCN8A (Nav1.6): Properties and de novo mutations in epileptic encephalopathy and intellectual disability. *Front Genet* 4:213.
2. Maier SK, et al. (2004) Distinct subcellular localization of different sodium channel alpha and beta subunits in single ventricular myocytes from mouse heart. *Circulation* 109(11):1421–1427.
3. Maier SK, et al. (2002) An unexpected role for brain-type sodium channels in coupling of cell surface depolarization to contraction in the heart. *Proc Natl Acad Sci USA* 99(6): 4073–4078.
4. Noujaim SF, et al. (2012) A null mutation of the neuronal sodium channel NaV1.6 disrupts action potential propagation and excitation-contraction coupling in the mouse heart. *FASEB J* 26(1):63–72.
5. Poulet C, et al. (2015) Late sodium current in human atrial cardiomyocytes from patients in sinus rhythm and atrial fibrillation. *PLoS One* 10(6):e0131432.
6. Mishra S, et al. (2015) Contribution of sodium channel neuronal isoform Nav1.1 to late sodium current in ventricular myocytes from failing hearts. *J Physiol* 593(6): 1409–1427.
7. Veeramah KR, et al. (2012) De novo pathogenic SCN8A mutation identified by whole-genome sequencing of a family quartet affected by infantile epileptic encephalopathy and SUDEP. *Am J Hum Genet* 90(3):502–510.
8. Wagnon JL, Meisler MH (2015) Recurrent and non-recurrent mutations of SCN8A in epileptic encephalopathy. *Front Neurol* 6:104.
9. Carvill GL, et al. (2013) Targeted resequencing in epileptic encephalopathies identifies de novo mutations in CHD2 and SYNGAP1. *Nat Genet* 45(7):825–830.
10. Larsen J, et al.; EuroEPINOMICS RES Consortium CRP (2015) The phenotypic spectrum of SCN8A encephalopathy. *Neurology* 84(5):480–489.
11. Mercimek-Mahmutoglu S, et al. (2015) Diagnostic yield of genetic testing in epileptic encephalopathy in childhood. *Epilepsia* 56(5):707–716.
12. Allen AS, et al.; Epi4K Consortium; Epilepsy Phenome/Genome Project (2013) De novo mutations in epileptic encephalopathies. *Nature* 501(7466):217–221.
13. Trump N, et al. (2016) Improving diagnosis and broadening the phenotypes in early-onset seizure and severe developmental delay disorders through gene panel analysis. *J Med Genet* 53(5):310–317.
14. Estacion M, et al. (2014) A novel de novo mutation of SCN8A (Nav1.6) with enhanced channel activation in a child with epileptic encephalopathy. *Neurobiol Dis* 69: 117–123.
15. Kong W, et al. (2015) SCN8A mutations in Chinese children with early onset epilepsy and intellectual disability. *Epilepsia* 56(3):431–438.
16. Blanchard MG, et al. (2015) De novo gain-of-function and loss-of-function mutations of SCN8A in patients with intellectual disabilities and epilepsy. *J Med Genet* 52(5): 330–337.
17. de Kovel CG, et al. (2014) Characterization of a de novo SCN8A mutation in a patient with epileptic encephalopathy. *Epilepsy Res* 108(9):1511–1518.
18. Wagnon JL, et al. (2015) Pathogenic mechanism of recurrent mutations of SCN8A in epileptic encephalopathy. *Ann Clin Transl Neurol* 3(2):114–123.
19. Lopez-Santiago L, et al. (2015) A mouse model of a human SCN8A epileptic encephalopathy mutation exhibits increased persistent sodium current in bipolar and pyramidal hippocampus neurons. *Proceedings of the American Epilepsy Society Annual Meeting*, p 3.142.
20. Yuan Y, et al. (2015) Abnormal firing activity in hippocampal neurons from a mouse model of SCN8A epileptic encephalopathy *Proceedings of the American Epilepsy Society Annual Meeting*, p 2.114.
21. Hesdorffer DC, et al.; ILAE Commission on Epidemiology; Subcommission on Mortality (2011) Combined analysis of risk factors for SUDEP. *Epilepsia* 52(6):1150–1159.
22. Dravet C, Oguni H (2013) Dravet syndrome (severe myoclonic epilepsy in infancy). *Handb Clin Neurol* 111:627–633.
23. Auerbach DS, et al. (2013) Altered cardiac electrophysiology and SUDEP in a model of Dravet syndrome. *PLoS One* 8(10):e77843.
24. Kalume F, et al. (2013) Sudden unexpected death in a mouse model of Dravet syndrome. *J Clin Invest* 123(4):1798–1808.
25. Lopez-Santiago LF, et al. (2007) Sodium channel Scn1b null mice exhibit prolonged QT and RR intervals. *J Mol Cell Cardiol* 43(5):636–647.
26. Lin X, et al. (2015) Scn1b deletion leads to increased tetrodotoxin-sensitive sodium current, altered intracellular calcium homeostasis and arrhythmias in murine hearts. *J Physiol* 593(6):1389–1407.
27. Jones JM, Meisler MH (2014) Modeling human epilepsy by TALEN targeting of mouse sodium channel Scn8a. *Genesis* 52(2):141–148.
28. Wagnon JL, et al. (2015) Convulsive seizures and SUDEP in a mouse model of SCN8A epileptic encephalopathy. *Hum Mol Genet* 24(2):506–515.
29. Cerrone M, et al. (2005) Bidirectional ventricular tachycardia and fibrillation elicited in a knock-in mouse model carrier of a mutation in the cardiac ryanodine receptor. *Circ Res* 96(10):e77–e82.
30. Zhao YT, et al. (2015) Arrhythmogenesis in a catecholaminergic polymorphic ventricular tachycardia mutation that depresses ryanodine receptor function. *Proc Natl Acad Sci USA* 112(13):E1669–E1677.
31. Plummer NW, et al. (1998) Exon organization, coding sequence, physical mapping, and polymorphic intragenic markers for the human neuronal sodium channel gene SCN8A. *Genomics* 54(2):287–296.
32. Santiago DJ, et al. (2010) Ca sparks do not explain all ryanodine receptor-mediated SR Ca leak in mouse ventricular myocytes. *Biophys J* 98(10):2111–2120.
33. Dhar Malhotra J, et al. (2001) Characterization of sodium channel alpha- and beta-subunits in rat and mouse cardiac myocytes. *Circulation* 103(9):1303–1310.
34. Duclohier H (2005) Neuronal sodium channels in ventricular heart cells are localized near T-tubules openings. *Biochem Biophys Res Commun* 334(4):1135–1140.
35. Massey CA, Sowers LP, Dlouhy BJ, Richerson GB (2014) Mechanisms of sudden unexpected death in epilepsy: The pathway to prevention. *Nat Rev Neurol* 10(5):271–282.
36. Finsterer J, Wahbi K (2014) CNS-disease affecting the heart: Brain-heart disorders. *J Neurol Sci* 345(1-2):8–14.
37. Smithson WH, Colwell B, Hanna J (2014) Sudden unexpected death in epilepsy: Addressing the challenges. *Curr Neurol Neurosci Rep* 14(12):502.
38. Genton P, Velizarova R, Dravet C (2011) Dravet syndrome: The long-term outcome. *Epilepsia* 52(Suppl 2):44–49.
39. Sakauchi M, et al. (2011) Retrospective multiinstitutional study of the prevalence of early death in Dravet syndrome. *Epilepsia* 52(6):1144–1149.
40. Surges R, et al. (2010) Pathologic cardiac repolarization in pharmacoresistant epilepsy and its potential role in sudden unexpected death in epilepsy: A case-control study. *Epilepsia* 51(2):233–242.
41. Surges R, Thijs RD, Tan HL, Sander JW (2009) Sudden unexpected death in epilepsy: Risk factors and potential pathomechanisms. *Nat Rev Neurol* 5(9):492–504.
42. Shorvon S, Tomson T (2011) Sudden unexpected death in epilepsy. *Lancet* 378(9808): 2028–2038.
43. Schuele SU, et al. (2007) Video-electrographic and clinical features in patients with ictal asystole. *Neurology* 69(5):434–441.
44. Schuele SU, Widdess-Walsh P, Bermeo A, Lüders HO (2007) Sudden unexplained death in epilepsy: The role of the heart. *Cleve Clin J Med* 74(Suppl 1):S121–S127.
45. Sandorfi G, Clemens B, Csanadi Z (2013) Electrical storm in the brain and in the heart: Epilepsy and Brugada syndrome. *Mayo Clin Proc* 88(10):1167–1173.
46. Gautier NM, Glasscock E (2015) Spontaneous seizures in Kcna1-null mice lacking voltage-gated Kv1.1 channels activate Fos expression in select limbic circuits. *J Neurochem* 135(1):157–164.
47. Moore BM, et al. (2014) The Kv1.1 null mouse, a model of sudden unexpected death in epilepsy (SUDEP). *Epilepsia* 55(11):1808–1816.
48. Partemi S, et al. (2013) Loss-of-function KCNH2 mutation in a family with long QT syndrome, epilepsy, and sudden death. *Epilepsia* 54(8):e112–e116.
49. Zamorano-León JJ, et al. (2012) KCNH2 gene mutation: A potential link between epilepsy and long QT-2 syndrome. *J Neurogenet* 26(3-4):382–386.
50. Tu E, Bagnall RD, Duflou J, Semsarian C (2011) Post-mortem review and genetic analysis of sudden unexpected death in epilepsy (SUDEP) cases. *Brain Pathol* 21(2): 201–208.
51. Johnson JN, et al. (2009) Identification of a possible pathogenic link between congenital long QT syndrome and epilepsy. *Neurology* 72(3):224–231.
52. Goldman AM, et al. (2009) Arrhythmia in heart and brain: KCNQ1 mutations link epilepsy and sudden unexplained death. *Sci Transl Med* 1(2):2ra6.
53. Møller RS, et al. (2015) Mutations in KCNT1 cause a spectrum of focal epilepsies. *Epilepsia* 56(9):e114–e120.
54. Tu E, Waterhouse L, Duflou J, Bagnall RD, Semsarian C (2011) Genetic analysis of hyperpolarization-activated cyclic nucleotide-gated cation channels in sudden unexpected death in epilepsy cases. *Brain Pathol* 21(6):692–698.
55. Nava C, et al.; EuroEPINOMICS RES Consortium (2014) De novo mutations in HCN1 cause early infantile epileptic encephalopathy. *Nat Genet* 46(6):640–645.
56. Qi Y, et al. (2014) Hyper-SUMOylation of the Kv7 potassium channel diminishes the M-current leading to seizures and sudden death. *Neuron* 83(5):1159–1171.
57. Biet M, et al. (2015) Prolongation of action potential duration and QT interval during epilepsy linked to increased contribution of neuronal sodium channels to cardiac late Na+ current: Potential mechanism for sudden death in epilepsy. *Circ Arrhythm Electrophysiol* 8(4):912–920.
58. Matsuki N, Hermsmeyer K (1983) Tetrodotoxin-sensitive Na+ channels in isolated single cultured rat myocardial cells. *Am J Physiol* 245(5 Pt 1):C381–C387.
59. Westenbroek RE, et al. (2013) Localization of sodium channel subtypes in mouse ventricular myocytes using quantitative immunocytochemistry. *J Mol Cell Cardiol* 64:69–78.
60. Radwański PB, et al. (2015) Neuronal Na+ channel blockade suppresses arrhythmogenic diastolic Ca2+ release. *Cardiovasc Res* 106(1):143–152.
61. Torres NS, Larbig R, Rock A, Goldhaber JI, Bridge JH (2010) Na+ currents are required for efficient excitation-contraction coupling in rabbit ventricular myocytes: A possible contribution of neuronal Na+ channels. *J Physiol* 588(Pt 21):4249–4260.
62. Velagapudi P, Turagam M, Laurence T, Kocheril A (2012) Cardiac arrhythmias and sudden unexpected death in epilepsy (SUDEP). *Pacing Clin Electrophysiol* 35(3): 363–370.
63. Dybkova N, et al. (2014) Tubulin polymerization disrupts cardiac β-adrenergic regulation of late INa. *Cardiovasc Res* 103(1):168–177.
64. Chen J, et al. (2016) Cardiac sodium channel mutation associated with epinephrine-induced QT prolongation and sinus node dysfunction. *Heart Rhythm* 13(1):289–298.
65. Tomko SR, Mirsa SN, Coorg R, Wilfong A (2015) A case of recurrent asystole associated with seizures responding to sodium channel inhibition in an infant with novel SCN8A mutation. *Proceedings of the American Epilepsy Society Annual Meeting*, p 1.381.